Advanced Quantum Effects Simulation in *ATLAS*

Introduction

The trend toward smaller MOSFET devices with thinner gate oxide and greater doping is resulting in the increased importance of quantum mechanical effects, which are observed as shifts in threshold voltage and gate capacitance. Predicting these quantum effects requires solving the Schrodinger equation. This article presents the Poisson-Schrodinger solver and recent enhancements implemented in ***ATLAS*** from Silvaco.

Schrodinger-Poisson

To model the effects of quantum confinement, ***Quantum*** allows the self-consistent solution of the Schrodinger equation with Poisson's equation. Poisson's equation is solved in two dimensions over the entire device while Schrodinger's equation is solved in one dimensional slices across the device.

These solutions provide calculations of the bound sate energies (Eigen energies), the carrier wave functions (Eigen functions), and carrier concentrations in the presence of quantum mechanical confining potential variations.

Considering ml, mt1 and mt2 the electron longitudinal effective mass and the electron transverse effective masses respectively, the electron density is written as:

$$n(x) = \frac{2k_B T}{\pi\hbar^2}$$

$$\left\{\sqrt{m_l m_{t1}}\sum_i \left|\Psi_{li}(x)\right|^2 \ln\left[1+\exp\frac{E_F - E_{li}}{k_B T}\right]\right.$$

$$+\sqrt{m_l m_{t2}}\sum_i \left|\Psi_{t1i}(x)\right|^2 \ln\left[1+\exp\frac{E_F - E_{t1i}}{k_B T}\right]$$

$$\left.+\sqrt{m_{t1} m_{t2}}\sum_i \left|\Psi_{t2i}(x)\right|^2 \ln\left[1+\exp\frac{E_F - E_{t2i}}{k_B T}\right]\right\}$$

where x is the position along a vertical slice (normal to the gate oxide), Ψ_{li}, E_{li} (resp. Ψ_i, E_{ti}) are the i-th longitudinal (resp. transverse) eigenvector and eigenvalue, k_B is the Boltzmann constant, T is the temperature, h is the Planck constant and E_F is the Fermi level. For the holes, a similar expression is obtained with the light and heavy holes effective masses.

	2D Poisson 1D Schrodinger	2D Poisson 2D Schrodinger	3D Poisson 2D Schrodinger
Regular Grid	X	X	X
Unstructured Grid	X		
Post Processing	X		
Non-Equilibrius	X	X	X
Strained Silicon	X	X	X
Radiative Models	X		X

Table 1. Schrodinger Poisson Operational Modes

Operational Modes

In ***Quantum***, solutions to the Schrodinger-Poisson system are used in various modes to accommodate various applications. The table above summarizes these modes.

Table 1 shows that ***Quantum*** offers three basic operational modes of solutions to the Schrodinger-Poisson system of equations: one-dimensional Schrodinger "slices" embedded in a two-dimensional Poisson solution mesh, two-dimensional Schrodinger solutions on the same two-dimensional Poisson solution mesh and two-dimensional Schrodinger "plane slices" embedded in a three-dimensional Poisson solution mesh.

For the rectangular grid approach, the grid points used for the Schrodinger solution exactly coincide with the grid points used in the Poisson solution. These solutions have the best self-consistency since they involve no interpolation between the Schrodinger and Poisson solution grids. Conversely, the unstructured grid approach requires a separate grid definition for the Schrodinger solution from the Poisson grid. This requires interpolation between the grids, but offers the advantage of allowing self-consistent S-P solutions for unstructured meshes such as are generated by the process simulator ***ATHENA*** or the interactive general purpose structure creation tool ***DevEdit***.

The post-processing approach does not solve Schrodinger's and Poisson's equation self-consistently. Instead Poisson's equation is solved self-consistently with the electron and hole continuity equations in the standard drift-diffusion approach. The Schrodinger solutions are then obtained using the classical Poisson solutions. This has the advantages of providing fast solutions and solutions can be taken far from zero bias (i.e. with currents flowing).

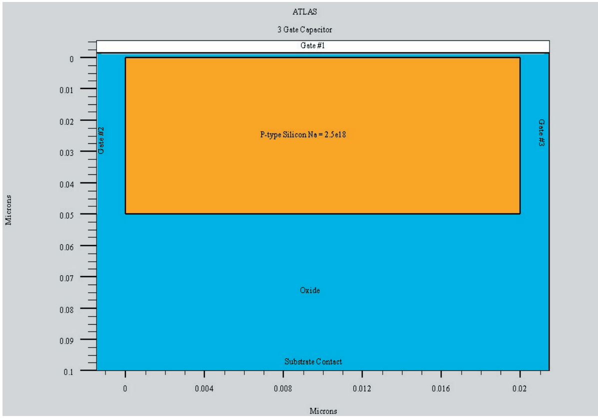

Figure 1. 3 gate capacitor.

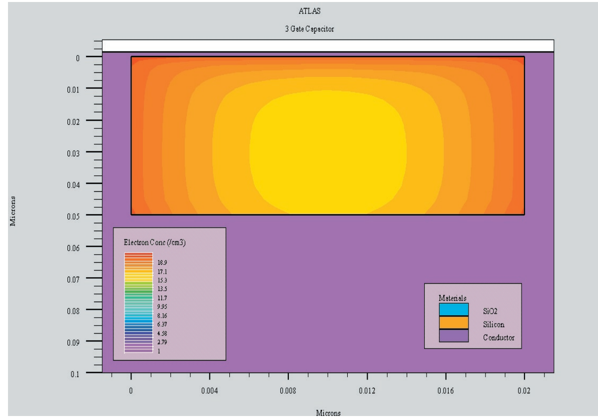

Figure 3. Classical electron concentration.

In the non-equilibrium mode, ***Quantum*** first calculates the self-consistent solution of Poisson's equation with the electron and hole continuity equations as in the standard drift-diffusion model. The Schrodinger-Poisson solutions are then calculated self-consistently using the quasi-Fermi levels from the classical solutions to estimate the non-classical carrier concentrations. This has advantages similar to the post-processing approach but gives self-consistent S-P solutions.

The strained silicon model provides for strain induced splitting in the conduction and valence bands in the solution of Schrodinger's equation.

For radiative modeling, ***Quantum*** provides Schrodinger-Poisson solutions to obtain bound state eigen energies which are used in the calculation of the momentum matrix elements. The Schrodinger-Poisson solutions also give the wave functions which can be used to calculate overlap integrals. The momentum matrix elements and overlap integrals are used in the calculation gain spectra (for lasers) and spontaneous emission spectra (for all light emission devices).

Two-Dimensional Schrodinger-Poisson Example

To demonstrate the two-dimensional Schrodinger-Poisson solver we constructed a simple 3 gate capacitor to demonstrate charge confinement in two dimensions. The device, shown in Figure 1, is composed of a heavily doped p-type silicon region completely embedded in silicon dioxide. Gates are placed at the top and either end of the silicon region. A substrate contact is at the bottom.

Figure 2 shows a contour plot of the electron concentration when the gates are biased to 0.5 V. In the figure and the zoomed inset the effects of quantum confinement can be clearly seen.

This can be contrasted with the classical solution shown in Figure 3.

Conclusion

The ***ATLAS*** Quantum model offers a variety of operational modes to accommodate a range of applications to address the effect of quantum confinement.

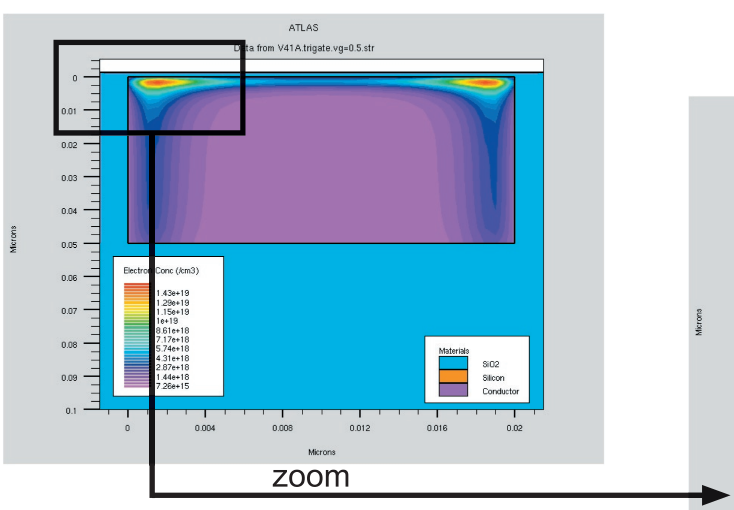

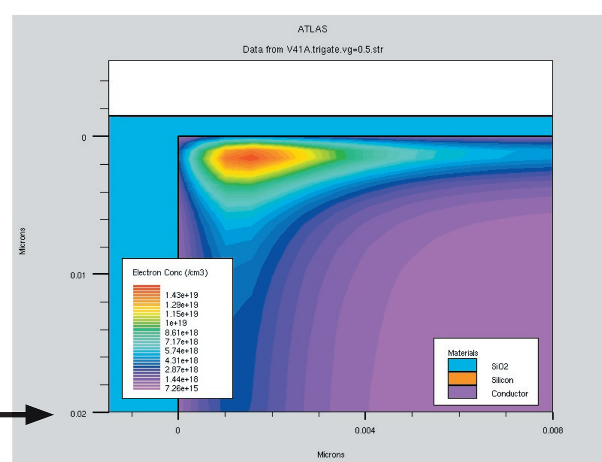

Figure 2 show electrons concentration in linear scale at Vgate=0.5V